Networked Microgrid Dynamic Formation for Optimal Load Restoration By Data-driven Distributionally Robust Optimization

Haonan Zhu[1], Chia-Chi Chu[2*], Pengfeng Lin[1], Wenping Qin[3], Miao Zhu[1], Peng Wang[4]
[1] Department of Electrical Engineering, *Shanghai Jiao Tong University*, Shanghai
[2] Department of Electrical Engineering, *National Tsing Hua University*, Taiwan
[3] College of Electrical and Power Engineering, *Taiyuan University of Technology*, Taiyuan
[4] School of Electrical and Automation Engineering, *Nanjing Normal University*, Nanjing
Email: zhn_kk6@sjtu.edu.cn, ccchu@ee.nthu.edu.tw, pengfeng_lin@sjtu.edu.cn, qinwenping@tyut.edu.cn, miaozhu@sjtu.edu.cn, epwang@ntu.edu.sg

***Abstract*—This paper presents a data-driven distributionally robust framework for post-disaster networked microgrid (NMG) formation that accounts for renewable generation uncertainty. The NMG formation model jointly determines time-varying MG topologies, the placement and dispatch of mobile distributed generators (DGs) and energy storage (ES), and the scheduling of dispatchable loads to maximize weighted critical load restoration. Line losses from a linearized DistFlow model are included in the objective function, and a resilience index is used to ensure sufficient DG reserve for assigned critical loads. Uncertainty in RES outputs is handled by distributionally robust chance constraints (DRCC) defined on a Wasserstein ambiguity set, and the DRCC is reformulated through a CVaR-based tractable approximation. The efficiency of the proposed model is verified by numerical simulations on a modified IEEE 33-node system.**

***Index Terms*—Distributionally robust chance constraints, resilience enhancement, AC microgrid (MG), mobile emergency resource (MER).**

I. Introduction

In recent decades, increasing environmental awareness and concerns about carbon emissions have led many regions worldwide to integrate renewable energy sources (RESs) and energy storage (ES) into distribution power grids [1]. However, as RES and ES penetration increases, conventional grid structures encounter operational challenges that threaten centralized coordination. Microgrids (MGs) have emerged as a solution, offering a way to integrate various distributed energy resources (DERs) into the distribution system, enhancing grid resilience [2] [3]. As MGs become electrically interconnected and functionally interactive, the concept has expanded into Networked Microgrids (NMGs), which can operate independently, sustain critical loads, and ultimately enhance resilience through local control and rapid response [4] [5].

This study focuses on post-disaster grid reconstruction using NMGs to enhance distribution system resilience. Traditional feeder reconfiguration methods [6] [7] mainly minimize power losses under normal conditions but may fail after severe incidents when upstream substations or lines are damaged. To address this limitation, the proposed strategy dynamically forms sub-MGs around DGs and Mobile Emergency Resources (MERs), restoring critical loads (CLs) through flexible topology reconfiguration immediately after the disconnection from upstream substations [8]. The NMG formation problem is formulated to determine feasible typologies, as well as the placement and dispatch of mobile DGs and ESs, to maximize the weighted restoration of CLs [9] [10].

To address the uncertainty of RES, the NMG formulation will be extended to distributionally robust optimization (DRO) formulation, where the uncertainty of forecasting RES can be described by an ambiguous probability distribution [11]. Since only the uncertainty range—not exact data—is known, this may lead to biased optimization results. A common approach to mitigate this issue is to use ambiguous probability distributions to model the likelihood of different scenarios and incorporate as many scenarios as possible into the ambiguity set. This leads to a Data-Driven Distributionally Robust Optimization (D-DDRO) problem, which leverages statistical information and overcomes the conservatism of traditional robust optimization [12].

In this paper, a distributionally robust chance-constrained (DRCC) formulation is adopted as a specific implementation of D-DDRO to model stochastic RES outputs [13]. The DRCC formulation provides a balance between reliability and operational flexibility, avoiding overly conservative dispatch decisions [14]. However, the key challenge lies in reformulating the DRCC over the uncertain probability distribution within the ambiguity set. This study uses the Wasserstein metric-based ambiguity set to measure the similarity between probability distributions, ensuring the desired level of accuracy [12]. Unlike conventional robust optimization methods that focus on avoiding the worst-case scenario, the worst-case expectation problem in DRCC can be solved in its dual form [15]. Numerical simulations of two NMGs will be conducted to demonstrate the effectiveness of the proposed scheme.

This work was supported by the National Natural Science Foundation of China under Grant No. 52507124. (Corresponding author: Chia-Chi Chu.)

979-8-3315-8138-1

The paper will be organized as follows: Sec. I presents the background and literature review. Sec. II outlines the general problem formulation for NMG formation resilience enhancement. Sec. III discusses model descriptions with uncertainties and employs DRCC techniques to solve the problem. Sec. IV provides comprehensive simulation results on a modified IEEE 33-node system to validate the proposed resilience enhancement scheme, while Sec. V concludes the study.

II. Problem Formulation

After extreme events, damage to substations or feeders may isolate the distribution system from the main grid. To maintain supply to CLs, the network must be reconfigured into multiple MGs. A set of mobile DGs and ESs, denoted as $\mathcal{K}$ and $\mathcal{S}$ respectively, are deployed to support network restoration. As the output of RESs fluctuates over time, MG topology is dynamically adjusted through switch operations for flexible and coordinated operation.

A. Objective function

The objective of NMG formation problem is defined below to maximize the total critical load that can be restored:

$$\max_{s^{i,t}} \sum_{t\in\mathcal{T}}\sum_{i\in\mathcal{N}} w^i s^{i,t} p^i, \tag{1}$$

where w^i represents a pre-defined weight factor for each load, $s^{i,t}$ is a binary state variable indicating whether load is restored at time t and p^i denotes the real power at load node i.

B. Constraints

The NMG formation problem is subjected to three types of constraints:

1) Micogrid topology constraints

$$\sum_{k\in\mathcal{K}} v^{k,i,t} = 1,\ \forall i\in\mathcal{N}, t\in\mathcal{T} \tag{2}$$

$$\sum_{k\in\mathcal{K}} z^{k,i}\ \le 1, \forall i\in\mathcal{N},\ \sum_{i\in\mathcal{N}} z^{k,i}\ = 1, \forall k\in\mathcal{K} \tag{3}$$

$$\sum_{i\in\mathcal{N}} u^{s,i} = 1,\ \forall s\in\mathcal{S},\ \sum_{s\in\mathcal{S}} u^{s,i} \le 1,\ \forall i\in\mathcal{N} \tag{4}$$

$$v^{k,i,t} \ge z^{k,i},\ \forall k\in\mathcal{K}, i\in\mathcal{N}, t\in\mathcal{T} \tag{5}$$

$$c_{ij}^{k,t} \le v^{k,i,t}, \forall k\in\mathcal{K}, (i,j)\in\mathcal{L}, t\in\mathcal{T} \tag{6}$$

$$c_{ij}^{k,t} \le v^{k,j,t}, \forall k\in\mathcal{K}, (i,j)\in\mathcal{L}, t\in\mathcal{T} \tag{7}$$

$$c_{ij}^{k,t} \ge v^{k,i,t} + v^{k,j,t} - 1, \forall k\in\mathcal{K}, (i,j)\in\mathcal{L}, t\in\mathcal{T} \tag{8}$$

$$b_{ij}^t = \sum_{k\in\mathcal{K}} c_{ij}^{k,t},\ \forall (i,j)\in\mathcal{L}, t\in\mathcal{T} \tag{9}$$

where $v^{k,i,t}$ represents the binary state variable for node i belonging to MG$_k$; $z^{k,i}$ and $u^{s,i}$ indicate the connections of DGk and ESs to node i respectively; b_{ij}^t and $c_{ij}^{k,t}$ represent the switch state and the MG$_k$ assignment of line (i,j). As the goal is to serve as many critical loads as possible, each node must be assigned to a MG, as shown in (2). Constraints (3) and (4) ensure that each DG and ES unit is connected to one node, and each node has at most one such device. Constraint (5) ensures that each DG is assigned to its respective surrounding nodes to form a MG. Constraints (6)–(8) ensure that a line can be assigned to MG only if both of its nodes belong to that MG. Constraint (9) indicates that line switch will be forced open when its nodes are not allocated to the same MG.

2) Output constraints

$$\sum_{k\in\mathcal{K}} z^{k,i} P_{\min}^k \le P_{dg}^{i,t} \le \sum_{k\in\mathcal{K}} z^{k,i} P_{\max}^k,\ \forall i\in\mathcal{N}, t\in\mathcal{T} \tag{10}$$

$$\sum_{k\in\mathcal{K}} z^{k,i} Q_{\min}^k \le Q_{dg}^{i,t} \le \sum_{k\in\mathcal{K}} z^{k,i} Q_{\max}^k,\ \forall i\in\mathcal{N}, t\in\mathcal{T} \tag{11}$$

$$P_{res,\min}^{r,i} \le P_{res}^{r,i,t} \le P_{res,\max}^{r,i},\ \forall r\in\mathcal{R}, i\in\mathcal{N}, t\in\mathcal{T} \tag{12}$$

$$Q_{res,\min}^{r,i} \le Q_{res}^{r,i,t} \le Q_{res,\max}^{r,i},\ \forall r\in\mathcal{R}, i\in\mathcal{N}, t\in\mathcal{T} \tag{13}$$

$$0 \le P_{ch}^{i,t} \le \sum_{s\in\mathcal{S}} u^{s,i} P_{ch,\max}^s\ \mu_{ch}^{s,t},\ \forall i\in\mathcal{N}, t\in\mathcal{T} \tag{14}$$

$$0 \le P_{dch}^{i,t} \le \sum_{s\in\mathcal{S}} u^{s,i} P_{dch,\max}^s\ \mu_{dch}^{s,t},\ \forall i\in\mathcal{N}, t\in\mathcal{T} \tag{15}$$

$$\mu_{ch}^{s,t} + \mu_{dch}^{s,t} \le 1,\ \forall s\in\mathcal{S}, t\in\mathcal{T} \tag{16}$$

$$E_{es}^{s,t} = E_{es}^{s,t-1} + P_{ch}^{s,t}\Delta t\eta_{ch} - P_{dch}^{s,t}\Delta t/\eta_{dch},\ \forall s\in\mathcal{S}, t\in\mathcal{T}\backslash\{0\} \tag{17}$$

$$E_{es,\min}^s \le E_{es}^{s,t} \le E_{es,\max}^s,\ \forall s\in\mathcal{S}, t\in\mathcal{T} \tag{18}$$

$$E_{es}^{s,T} = E_{es}^{s,0},\ \forall s\in\mathcal{S} \tag{19}$$

where $P_{dg}^{i,t}, Q_{dg}^{i,t}, P_{res}^{r,i,t}, Q_{res}^{r,i,t}$ represent the active and reactive power output of DG ans RES. $P_{ch}^{i,t}, P_{dch}^{i,t}, \mu_{ch}^{s,t}, \mu_{dch}^{s,t}$ and $E_{es}^{s,t}$ represent charging/discharging power, binary state variable and energy level of ES. The active and reactive power output of DGs and RESs are shown in (10)-(13). Constraints (14) and (15) depict the charging and discharging powers of ES, while Constraint (16) ensures that it cannot charge and discharge at the same time. Constraint (17) describes the energy balance of the ES, linking its energy level to charging and discharging power. Constraint (18) bounds the energy level of ES and (19) ensures it restore to initial state.

3) Operation constraints

$$\sum_{j:(j,i)\in\mathcal{L}} P_{ji}^t - \sum_{j:(i,j)\in\mathcal{L}} P_{ij}^t + P_G^{i,t} - s^{i,t}p^i = 0,\ \forall i\in\mathcal{N}, t\in\mathcal{T} \tag{20}$$

$$\sum_{j:(j,i)\in\mathcal{L}} Q_{ji}^t - \sum_{j:(i,j)\in\mathcal{L}} Q_{ij}^t + Q_G^{i,t} - s^{i,t}q^i = 0,\ \forall i\in\mathcal{N}, t\in\mathcal{T} \tag{21}$$

$$P_G^{i,t} = P_{dg}^{i,t} + P_{res}^{i,t} + P_{dch}^{i,t} - P_{ch}^{i,t},\ \forall i\in\mathcal{N}, t\in\mathcal{T} \tag{22}$$

$$Q_G^{i,t} = Q_{dg}^{i,t} + Q_{res}^{i,t},\ \forall i\in\mathcal{N}, t\in\mathcal{T}, \tag{23}$$

$$V_i^t = V_j^t + (r_{ij}P_{ij}^t + x_{ij}Q_{ij}^t)/V_o + \delta_{ij}^t, \forall (i,j)\in\mathcal{L}, t\in\mathcal{T} \tag{24}$$

$$\left(-1 + b_{ij}^t\right)V_o \le \delta_{ij}^t \le \left(1 - b_{ij}^t\right)V_o, \forall (i,j)\in\mathcal{L}, t\in\mathcal{T} \tag{25}$$

$$-T_{ij}^{P}b_{ij}^{t} \le P_{ij}^{t} \le T_{ij}^{P}b_{ij}^{t},\ \forall (i,j) \in \mathcal{L}, t \in \mathcal{T} \quad (26)$$

$$-T_{ij}^{Q}b_{ij}^{t} \le Q_{ij}^{t} \le T_{ij}^{Q}b_{ij}^{t},\ \forall (i,j) \in \mathcal{L}, t \in \mathcal{T} \quad (27)$$

$$V_i^t \le V_{\max} + \sum_{k \in \mathcal{K}} z^{k,i}(V_o - V_{\max}),\ \forall i \in \mathcal{N}, t \in \mathcal{T} \quad (28)$$

$$V_i^t \ge V_{\min} + \sum_{k \in \mathcal{K}} z^{k,i}(V_o - V_{\min}),\ \forall i \in \mathcal{N}, t \in \mathcal{T} \quad (29)$$

$$R^{k,t} = \frac{P_{DG}^{k} - \sum P_{Critical}^{i,t}}{P_{DG}^{k}} > R,\ \forall k \in \mathcal{K}, t \in \mathcal{T} \quad (30)$$

where $P_{ij}^t, Q_{ij}^t, P_G^{i,t}, Q_G^{i,t}, V_i^t$ represent the active and reactive power of line (i,j), node i and voltage at node i, respectively, δ_{ij}^t is a slack variable that relaxes the power flow constraint of line (i,j). For the power flow of the system, a DistFlow model is employed to mitigate the computational burden, which is shown in (20)-(25). Constraint (26) and (27) ensure that power transmission is only possible within upper and lower limits when the line switch is closed. Constraints (28) and (29) bound voltage for each node, and clamp to nominal voltage V_o for nodes connecting DGs. To ensure that DGs have enough capacity to serve CLs, a resilience metric R is introduced to assess the preparation of MGs, as shown in (30).

C. Model Refinements and Enhancements

To enhance resource allocation efficiency, a hybrid load approach is introduced: comprising both dispatchable loads p_d and non-dispatchable loads. Therefore, the objective function will be modified as follows:

$$\max_{s^{i,t}, p_d^{i,t}} \sum_{t \in \mathcal{T}} \sum_{i \in \mathcal{N}} w^i s^{i,t} p_d^{i,t} \quad (31)$$

where $p_d^{i,t}$ is confined by :

$$d^i p_{\mathrm{lb}}^i + \left(1 - d^i\right) p^i \le p_d^{i,t} \le p^i \quad (32)$$

where parameter d^i indicates whether the load at node i is dispatchable or not, as p_{lb}^i describes the minimum load to restore. However, due to $p_d^{i,t}$ and $s^{i,t}$ being control variables, the objective function becomes non-linear. To solve this issue, the active and reactive power service demand variable $p_s^{i,t}$ and $q_s^{i,t}$ are introduced:

$$p_s^{i,t} \le s^{i,t} p^i;\ 0 \le p_s^{i,t} \le p_d^{i,t};\ p_s^{i,t} \ge p_d^{i,t} - \left(1 - s^{i,t}\right) p^i \quad (33)$$

$$q_s^{i,t} = \frac{q^i}{p^i} p_s^{i,t},\ \forall i \in \mathcal{N}, t \in \mathcal{T},\ \text{and } p^i \ne 0 \quad (34)$$

Thus, these power flow equations (12) and (13) will be modified into the following linear equations:

$$\sum_{j:(j,i) \in \mathcal{L}} P_{ji}^t - \sum_{j:(i,j) \in \mathcal{L}} P_{ij}^t + P_G^{i,t} - p_s^{i,t} = 0,\ \forall i \in \mathcal{N}, t \in \mathcal{T} \quad (35)$$

$$\sum_{j:(j,i) \in \mathcal{L}} Q_{ji}^t - \sum_{j:(i,j) \in \mathcal{L}} Q_{ij}^t + Q_G^{i,t} - q_s^{i,t} = 0,\ \forall i \in \mathcal{N}, t \in \mathcal{T} \quad (36)$$

The predicted upper limit of RES active power in constraint (12) is inherently uncertain. To address it, Distributionally Robust Chance Constraint (DRCC) is adopted, ensuring that the constraint holds with a specified confidence level. The real power output of RES is described by the following DRCC:

$$\inf_{\mathbb{Q} \in D_W} \Pr\left[P_{res}^{i,t} - P_{res,\max}^{i,t} \le 0\right] \ge 1 - \epsilon \quad (37)$$

where D_W is the ambiguity set to describe the uncertain random variable $P_{res}^{i,t}$ and the risk parameter ϵ is the predefined allowable violation probability.

To further enhance the accuracy of network operation representation, line losses are incorporated into the objective function based on DistFlow model.

$$\max \sum_{t \in \mathcal{T}} \left(\sum_{i \in \mathcal{N}} w^i p_s^{i,t} - \sum_{(i,j) \in \mathcal{L}} r_{ij} \left(P_{ij}^2 + Q_{ij}^2\right) / V_o^2 \right) \quad (38)$$

Summarizing the aforementioned, the complete problem of NMG formation can be described as follows:

$$\max\ (38) \quad (39)$$

$$\text{s.t. } (2) - (30), (32) - (37) \quad (40)$$

III. Optimization Problem Reformation

The proposed NMG formation problem is computationally intractable with the DRCC. In this section, we introduce how to construct data-driven ambiguity sets and reformulate the DRCC to enable the NMG formation problem to be solved.

A. Wasserstein Metric Based Ambiguity Sets

This paper employs the Wasserstein metric to construct the ambiguity set. The Wasserstein metric between two distributions $\mathbb{Q}$ and $\mathbb{Q}_0$ is defined as follows:

$$d_W(\mathbb{Q} : \mathbb{Q}_0) = \inf \left(\int_{\Xi^2} \|\xi - \xi^0\| \, \Pi(\mathrm{d}\xi, \mathrm{d}\xi^0) \right) \quad (41)$$

where Ξ is the support set of multi-dimensional random variable $\xi \in \mathbb{R}^m$, Π is a joint distribution of ξ and ξ^0 with marginals $\mathbb{Q}$ and $\mathbb{Q}_0$.

The Wasserstein ambiguity set D_W is defined as a set comprising all underlying probability distributions that lie within a ball of radius θ, centered at the empirical distribution $\mathbb{Q}_0$.

$$D_W = \{\mathbb{Q} \in M(\Xi) : d_W(\mathbb{Q} : \mathbb{Q}_0) \le \theta\} \quad (42)$$

where $M(\Xi)$ represent all probability distributions $\mathbb{Q}$ supported on Ξ, $\Xi = \{C\xi \le d\}$.

The empirical distribution $\mathbb{Q}_0$ heavily relies on historical data, which can be specifically constructed from a set of data samples $\{\hat{\xi}_i\}_{i \in N}$,

$$\mathbb{Q}_0 = \frac{1}{N} \sum_{i=1}^{N} \delta_{\hat{\xi}_i} \quad (43)$$

where N represents the number of data samples, $\delta_{\hat{\xi}_i}$ represents the Dirac measure centered on $\hat{\xi}_i$.

B. Reformulation of DRCC

Since MG formation problem involving DRCC is generally difficult to solve, the original constraint must be reformulated

979-8-3315-8138-1

into a tractable form. For convenience, we consider the DRCC (37) in a general form:

$$\inf_{\mathbb{Q}\in D_W} \Pr_{\xi\sim\mathbb{Q}} \left[a(x)^T\xi \le b(x)\right] \ge 1-\epsilon \tag{44}$$

where $a(x)$ and $b(x)$ are affine functions on the optimization variable x.

The ambiguous chance constraint (44) cannot be solved computationally because the worst probability distribution $\mathbb{Q}$ is uncertain and infinite-dimensional. Therefore, we adopt the Conditional Value-at-Risk (CVaR) to obtain tractable approximations [16].

$$\begin{aligned}&\inf_{\mathbb{Q}\in D_W} \Pr_{\xi\sim\mathbb{Q}} \left[a(x)^T\xi \le b(x)\right] \ge 1-\epsilon\\ &\Leftrightarrow \sup_{\mathbb{Q}\in D_W} \mathbb{Q}-\text{CVaR}_\varepsilon\left(a(x)^T\xi - b(x)\right)\le 0\end{aligned} \tag{45}$$

where the CVaR at level ϵ for distribution $\mathbb{Q}$ is defined as:

$$\begin{aligned}&\mathbb{Q}-\text{CVaR}_\varepsilon\left(a(x)^T\xi - b(x)\right)\\ &\triangleq \inf_{\tau\in R}\left\{\tau+\frac{1}{\epsilon}\mathbb{E}_{\xi\sim\mathbb{Q}}\left[a(x)^T\xi-b(x)-\tau\right]^+\right\}\end{aligned} \tag{46}$$

where $[\theta]^+ = \max(\theta, 0)$.

By combining (45) and (46), the worst-case CVaR over the Wasserstein ambiguity set can be explicitly written as:

$$\begin{aligned}&\sup_{\mathbb{Q}\in D_W} \mathbb{Q}-\text{CVaR}_\varepsilon\left(a(x)^T\xi - b(x)\right)\\ &=\sup_{\mathbb{Q}\in D_W}\inf_{\tau\in R}\left\{\tau+\frac{1}{\epsilon}\mathbb{E}_{\xi\sim\mathbb{Q}}\left[a(x)^T\xi-b(x)-\tau\right]^+\right\}\\ &=\inf_{\tau\in R}\sup_{\mathbb{Q}\in D_W}\left\{\tau+\frac{1}{\epsilon}\mathbb{E}_{\xi\sim\mathbb{Q}}\left[a(x)^T\xi-b(x)-\tau\right]^+\right\}\end{aligned} \tag{47}$$

The sup and inf in (47) can be interchanged based on the stochastic saddle point theorem. The MG formation problem (39) can be reformulated as the following convex optimization problem [15]:

$$\begin{aligned}&\max\ (38)\\ &\text{s.t.}\quad \tau+\frac{1}{\epsilon}\left(\lambda\theta+\frac{1}{N}\sum_{i=1}^{N}s_i\right)\le 0\\ &\qquad a(x)\hat{\xi}_i-b(x)-\tau+\gamma_i^T\left(d-C^T\hat{\xi}_i\right)\le s_i\\ &\qquad \|C^T\gamma_i-a(x)\|_*\le\lambda, \gamma_i\ge 0, s_i\ge 0, \tau\in\mathbb{R}\\ &\qquad (2)-(30),(32)-(36)\end{aligned} \tag{48}$$

IV. Case Study

In this section, the proposed NMG formation problem is demonstrated on a modified IEEE 33-node system, which is shown in Fig. 1. Three RESs, modeled as photovoltaic units with diurnal generation patterns and output randomness, are employed at node 3, 24 and 28, respectively. Critical loads are selected from nodes with relatively higher demand and representative network locations, where loads at 10, 18 and 22 are assigned weight factor w_i of 2 and denoted as Critical load–2 and lodes at 14, 25 and 32 are assigned of 3 and denoted as Critical load–3. Loads at nodes 15, 20, 23 and 31 are defined as dispatchable loads. The time interval selected in the case is 1 hour, and the entire procedure is partitioned into 24 discrete time steps.

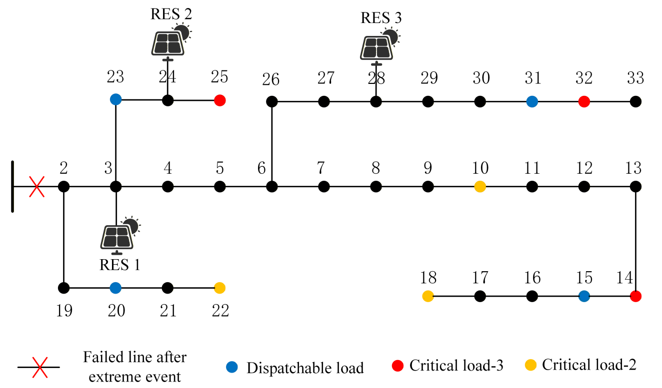

Fig. 1. The modified IEEE 33-node system.

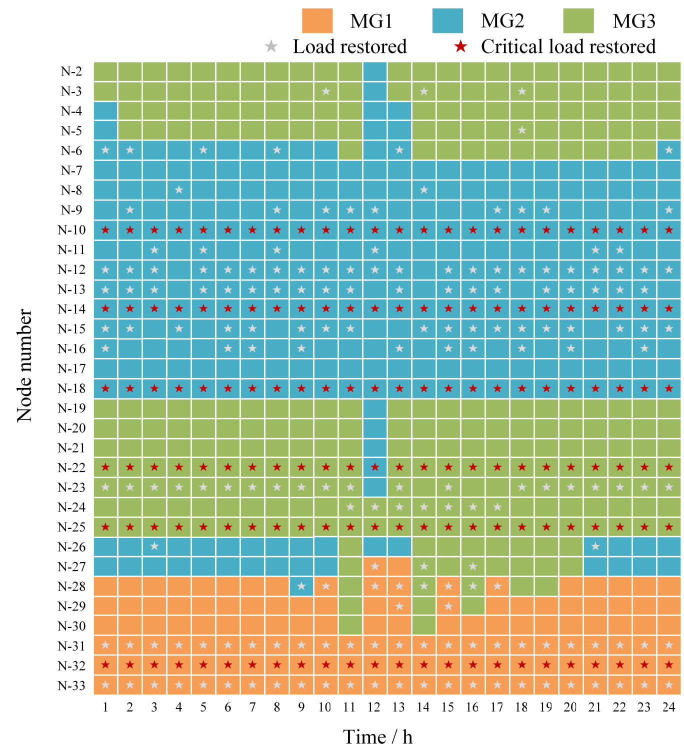

Fig. 2. Dynamic NMG formation result over 24 hours.

Simulations are conducted in Matlab using Gurobi 11.0.3 on an Intel Ultra5 125H PC (32GB RAM), with an average runtime of 726 seconds.

A. Optimization Results

As the simulation result shows, the distribution system is partitioned into three MGs through switch operations at each time step, due to the existence of three mobile DGs in the system, optimally positioned at node 32, 10 and 25 respectively. Two mobile ESs are placed at node 24 and 5, close to the RESs, to mitigate renewable generation fluctuations.

979-8-3315-8138-1

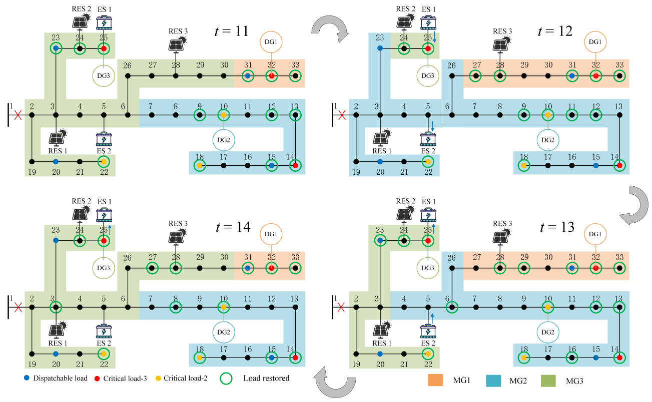

Fig. 3. System topology evolution from $t = 11$ to $t = 14$.

TABLE I
TOTAL WEIGHTED LOAD RESTORATION

	Method 1	Method 2	Method 3
Load(MW)	81.25	79.84	78.66

The load restored result of NMG formation problem is shown in Fig. 2, each node assigned to different MGs across time steps to maximize the total weighted load restoration. Specifically, the system prioritizes the recovery of all CLs. Even when the RES outputs vary over time, proper coordination of ESs and line switches ensures CLs' reliable supply.

Fig. 3 shows the evolution of system topology from $t = 11$ to $t = 14$. ES1 is charged before time step 11, so as to discharge at time step 12 to supply CL25 together with RES2 and DG3. At the same time, RES1 supports other loads and charges ES2 for prepare. At time step 13 and 14, ES2 and ES1 discharge to restore CLs at different MGs respectively. These results demonstrate that dynamic topology changes combined with storage coordination can improve the efficiency of CL's restoration.

B. Model Comparison

To further illustrate the performance of the proposed model, three cases are built and compared.

1) Method 1: The proposed DRCC NMG formation model, where network topology can vary along with time.
2) Method 2: A static DRCC NMG formation model, where the network topology remains static.
3) Method 3: A robust dynamic NMG formation model, where the uncertainty of RES outputs is addressed through robust optimization.

The total weighted load restoration of three method is shown in Table I. From Table I, it can be seen that the proposed DRCC-based dynamic NMG formation model achieves the highest restoration performance, increasing the total weighted load restoration by 1.76% and 3.29% compared with the static model and the robust optimization model respectively. This improvement demonstrates that the DRCC framework achieves superior restoration performance and resilience by balancing robustness and flexibility through worst-distribution considerations and dynamic topology reconfiguration.

V. CONCLUSION

This work develops a DRCC-based NMG formation method that integrates dynamic topology reconfiguration, mobile DG/ES placement and dispatch, and hybrid load handling. Incorporating line losses and a resilience index improves the operational realism, ensuring DGs hold adequate reserve for CLs. The Wasserstein-based ambiguity set is adopted to characterize the distributional uncertainty, while the CVaR reformulation transforms the DRCC into a tractable form that can be solved by commercial solvers. Numerical results on a modified IEEE 33-node test case show that proposed DRCC-based NMG formation method shows better restoration performance than a static topology and a traditional robust approach.

REFERENCES

[1] P. Lin, Q. Meng, M. Zhu, A. M. Y. M. Ghias, and F. Blaabjerg, "Dynamic Circuit-Based Unified Power Regulation for Hybrid AC/DC/DS Microgrids: A Comprehensive Approach to Static and Transient Control," *IEEE Trans. Ind. Electron.*, doi: 10.1109/TIE.2025.3585029.

[2] P. Lin, L. Du, H. Zhang, M. Zhu, J. Ma, and P. Wang, "Power lever: To transform interlinking architecture in hybrid ac/dc microgrids community," *IEEE Trans. Ind. Electron.*, 2025.

[3] E. I. E. Stasinos, D. N. Trakas, and N. D. Hatziargyriou, "Microgrids for power system resilience enhancement," *iEnergy*, vol. 1, no. 2, pp. 158-169, 2022.

[4] Z. Li, M. Shahidehpour, F. Aminifar, A. Alabdulwahab, and Y. Al-Turki, "Networked microgrids for enhancing the power system resilience," *Proc. IEEE*, vol. 105, no. 7, pp. 1289-1310, 2017.

[5] B. Chen, J. Wang, X. Lu, C. Chen, and S. Zhao, "Networked microgrids for grid resilience, robustness, and efficiency: A review," *IEEE Trans. Smart Grid*, vol. 12, no. 1, pp. 18-32, 2021.

[6] S. Poudel and A. Dubey, "Critical Load Restoration Using Distributed Energy Resources for Resilient Power Distribution System," *IEEE Trans. Power Syst.*, vol. 34, no. 1, pp. 52-63, Jan. 2019.

[7] J. Wen, W. Gan, C.-C. Chu, L. Jiang, and J. Luo, "Robust Resilience Enhancement by EV Charging Infrastructure Planning in Coupled Power Distribution and Transportation Systems", *IEEE Trans. Smart Grid*, vol. 16, no. 1, pp. 491-504, 2025.

[8] S. Cai, Y. Xie, Q. Wu, M. Zhang, X. Jin and Z. Xiang, "Distributionally Robust Microgrid Formation Approach for Service Restoration Under Random Contingency," *IEEE Trans. Smart Grid*, vol. 12, no. 6, pp. 4926-4937, Nov. 2021.

[9] S. Lei, J. Wang, C. Chen, and Y. Hou, "Mobile emergency generator prepositioning and real-time allocation for resilient response to natural disasters," *IEEE Trans. Smart Grid*, vol. 9, no. 3, pp. 2030–2041, May 2018.

[10] H. A. Abdelsalam, A. Eldosouky, and A. K. Srivastava, "Enhancing distribution system resiliency with microgrids formation using weighted average consensus," *Int. J. Electrical Power & Energy Systems*, vol. 141, pp. 108161, 2022.

[11] W. Wei and J. Wang, *Modeling and Optimization of Interdependent Energy Infrastructures*, Springer Nature, Switzerland, AG, 2020.

[12] X. A. Sun and A. J. Conejo, *Robust Optimization in Electric Energy Systems,* Int. Series in Operations Research & Management Science, vol. 313, Springer Nature, Switzerland AG, 2021.

[13] W. Jia, T. Ding, Y. Yuan, et al., "Decentralized distributionally robust chance-constrained operation of integrated electricity and hydrogen transportation networks," *Applied Energy*, vol. 377, pp. 124369, 2025.

[14] Z. Chen, D. Kuhn and W. Wiesemann, "Data-driven chance constrained programs over Wasserstein balls," *Operations Research*, vol. 72, no. 1, pp. 410-424, 2024.

[15] A. R. Hota, A. Cherukuri and J. Lygeros, "Data-Driven Chance Constrained Optimization under Wasserstein Ambiguity Sets," 2019 American Control Conference (ACC), Philadelphia, PA, USA, pp. 1501-1506, 2019.

[16] R. Rockafellar and S. Uryasev, "Optimization of conditional value-at-risk," *J. Risk*, vol. 2, no. 2, pp. 21–41, 1999.